Theoretical calculation of the cross sections of dielectronic recombination on He^+

Yu Zou,[1,2] Li-Bo Zhao,[1,3] and Quan-Yu Fang[2]
[1]*China Center for Advanced Science and Technology (World Laboratory), P.O. Box 8730, Beijing 100080, People's Republic of China*
[2]*Institute of Applied Physics and Computational Mathematics, P.O. Box 8009, Beijing 100088, People's Republic of China*
[3]*Department of Applied Physics, Beijing University of Aeronautics and Astronautics, Beijing 100083, People's Republic of China*
(Received 12 April 1999)

The relativistic multichannel theory has been applied to calculations of cross sections of dielectronic recombination on He^+. A first-order approximation is adopted for the radiative process. A correction based on isolated resonance approximation is used for the very narrow resonances among the $2lnl'$ states to include the radiation width. Twelve partial cross sections are calculated for both the $2lnl'$ and $3lnl'$ resonance states with $n \leqslant 5$. The convolved cross sections for the $n \leqslant 3$ states are in good agreement with those of the observations. A quantitative discrepancy for the $n=4$ and $n=5$ states may be attributed to the l dependence of the field ionization and the radiative decay during the time of flight. [S1050-2947(99)02611-6]

PACS number(s): 34.80.Kw, 32.90.+a, 32.80.Hd

I. INTRODUCTION

Dielectronic recombination (DR) [1] is an atomic process of practical importance and of fundamental physics interest [2–5]. In astrophysical and laboratory plasmas, DR can affect the ionization balance of plasmas, since this process makes the ionization degree of target ions change. It is also an important mechanism of energy loss of plasmas due to the emission of photons in the process. In order to study the kinetics in high-temperature plasmas, DR rates must be predicted accurately. In the fundamental research of atomic physics, DR provides us with a tool with which to study electron correlation, relativistic effects, and radiation damping. A great deal of doubly excited intermediate states are involved in DR processes. These states, especially the width of such states, are sensitive to electron correlation. It is well known that relativistic effects are important in heavy atoms. However, it was observed recently that the relativistic effects play a significant role in DR of the light C^{3+} ions [6]. The ''nonautoionizing'' terms $1s^2 2p4d\ ^3D$ and $1s^2 2p4f\ ^{1,3}F$, which are not expected to contribute to DR due to negligible overlap with the continuum, were quite surprising found to have the strongest DR resonance peaks. The effects of radiation damping have been seen in the electron-ion collisions [7]. However, it is prominent in the DR process [8].

The present work is an extension of our previous calculations on the doubly excited states of atomic helium [9]. In that work, the positions and widths of the doubly excited states $2spn^{\pm}$ and $2pnd$ in $^1P_1$ symmetry were calculated. Comparisons with the accurate photoabsorption experimental values showed good agreement in both the positions and the widths. The present extension is inspired by the experimental observation [10] of the DR cross sections on He^+, especially by that of the $\Delta n=2$ transition that involves $3lnl'$ resonance states. In this kind of transition, the isolated resonance approximation gives very poor results [11], since more Auger channels are possible while electron correlation is important. In the present calculations, the continuum wave functions of helium are computed with the relativistic multichannel theory (RMCT) [12,13] and the bound wave functions are obtained using the configuration interaction method. The radiative process is treated in the first-order approximation neglecting radiation width. For the $2lnl'(n \geqslant 3)$ resonance states, it is necessary to take into account the radiation width. A correction is made to the original calculated DR cross section assuming that the isolated resonance approximation is valid for such very narrow resonance states. The present results for both the $2lnl'$ and $3lnl'$ resonance states with $n \leqslant 3$ are in good agreement with the experimental measurement. A discrepancy exists for the resonance states with $n=4,5$ in both energy regimes. This discrepancy may be attributed to the field ionization that depends on both the angular momentum and principal quantum number of the outer electron. The radiative decay of the resonance states during the time of flight may affect the experimental measurements also. For the $3lnl'$ states, besides the $^3F^o$ term [10], which corresponds to total angular momentum and parity $J^\pi = 2^-$, 3^-, and 4^- in the present calculations, the symmetries with $J^\pi = 1^-$, 2^+, and 3^+ contribute significantly to the total DR cross sections.

II. THEORETICAL METHODS

The isolated resonance approximation is widely used in calculations of DR cross sections for various atomic systems. Several general methods have also been proposed for nonisolated resonance calculations [14–19]. Here, we only outline the theory of Davies, Bell, and Seaton (hereafter referred to be as DBS) [14,16] adopted in the present work, and our scheme to calculate DR within the framework of the RMCT.

A. The nonisolated resonance theory for dielectronic recombination

The DBS theory starts from the continuum wave function Ψ_{jE} and bound wave function Ψ_β of an atomic system excluding the radiative field. Based on the atomic wave functions, DR probability can be expressed as

$$P_j^{DR} = \sum_{\mu\beta} |\mathcal{S}_{\beta\mu,j}|^2, \tag{1}$$

with

$$S_{\beta\mu,j}=-2\pi i\sum_{\beta'\mu'}(1+\mathbf{L})^{-1}_{\beta\mu,\beta'\mu'}\cdot D_{j,\beta'\mu'}, \tag{2}$$

where matrix $\mathbf{L}$ is

$$\mathbf{L}(E)=\pi^2\mathbf{D}^{\dagger}(E)\mathbf{D}(E)-i\pi\mathrm{P}\int dE'\frac{\mathbf{D}^{\dagger}(E')\mathbf{D}(E')}{(E'-E)}, \tag{3}$$

and the P indicates the principal integral. The element of the radiative transition matrix $\mathbf{D}(E)$ is

$$D_{j,\beta\mu}(E)=\langle\Psi_{jE}|P^{(\mu)}|\Psi_{\beta}\rangle, \tag{4}$$

where $P^{(\mu)}$ is the dipole operator of radiative transitions with photon polarization μ.

For the doubly excited states of neutral atoms with the lower principal quantum number, the radiative width is much less important than the autoionization width. The first order theory with

$$S_{\beta\mu,j}=-2\pi iD_{j,\beta\mu} \tag{5}$$

is valid for these cases. In the present calculations for helium, we use the first order approximation to calculate the DR probabilities involving the doubly excited states $2lnl'$ and $3lnl'$ with $n\leqslant 5$. With the simple approximation for radiative process, we can focus on the calculation of the continuum wave function Ψ_{jE} in which electron correlation is very important. The configuration interaction expansion is adopted for the final bound wave function Ψ_{β}.

B. Continuum wave functions

Consider an atomic system with a Hamiltonian

$$H=H_0+V, \tag{6}$$

where

$$H_0=\sum_i\left[c\boldsymbol{\alpha}_i\cdot\mathbf{p}_i+\beta_imc^2+V_{SCF}(r_i)\right] \tag{7}$$

is the atomic self-consistent-field (SCF) Hamiltonian and

$$V=\sum_i\left[-\frac{Ze^2}{r_i}-V_{SCF}(r_i)\right]+\sum_{i>j}\frac{e^2}{r_{ij}} \tag{8}$$

is the residual interaction. In the present calculations, the Dirac-Fock-Slater approach is adopted to obtain the atomic SCF potential $V_{SCF}(r)$. The eigenvectors φ_n for discrete states and $\varphi_{j\epsilon}$ for continuum states of atomic SCF Hamiltonian H_0 form a basis set for atomic wave functions. These basis vectors are determined by

$$H_0\varphi_n=E_n^{(0)}\varphi_n, \tag{9a}$$

$$H_0\varphi_{j\epsilon}=\epsilon\varphi_{j\epsilon}. \tag{9b}$$

The finite vectors belonging to discrete configurations (φ_n) are included in the basis set explicitly and the infinite high Rydberg states as well as the continuum states ($\varphi_{j\epsilon}$) are treated as channels [12,13]. The vectors satisfy the orthogonalization conditions

$$\langle\varphi_n|\varphi_{n'}\rangle=\delta_{nn'}, \tag{10a}$$

$$\langle\varphi_{j\epsilon}|\varphi_{j'\epsilon'}\rangle=\delta_{jj'}\delta(\epsilon-\epsilon'), \tag{10b}$$

$$\langle\varphi_n|\varphi_{j\epsilon}\rangle=0. \tag{10c}$$

An eigenvector Ψ for the whole atomic system can be expanded as

$$\Psi=\sum_n A_n\varphi_n+\sum_i\int_{\epsilon_c}B_{i\epsilon}\varphi_{i\epsilon}d\epsilon, \tag{11}$$

with the coefficients A_n and $B_{j\epsilon}$ decided by

$$H\Psi=E\Psi. \tag{12}$$

Projecting on both sides of Eq. (12) with $\langle\varphi_{n'}|$ and $\langle\varphi_{i'E'}|$, respectively, gives

$$E_{n'}^{(0)}A_{n'}+\sum_n A_nV_{n',n}+\sum_i\int_{\epsilon_c}B_{i\epsilon}V_{n',i\epsilon}d\epsilon=EA_{n'}, \tag{13a}$$

$$E'B_{i'E'}+\sum_n A_nV_{i'E',n}+\sum_i\int_{\epsilon_c}B_{i\epsilon}V_{i'E',i\epsilon}d\epsilon=EB_{i'E'}, \tag{13b}$$

where $V_{n',n}=\langle\varphi_{n'}|V|\varphi_n\rangle$ is the matrix element for discrete-discrete configuration interactions, $V_{n',iE}=\langle\varphi_{n'}|V|\varphi_{iE}\rangle$ that for discrete-continuum interactions, $V_{i'E',iE}=\langle\varphi_{i'E'}|V|\varphi_{iE}\rangle$ that for continuum-continuum interactions. Since the residual interaction V is a short range potential obtained with the Dirac-Fock-Slater approach, the continuum-continuum interaction $V_{i'E',iE}$ as well as the discrete-continuum interaction $V_{n',iE}$ is convergent. In the derivation of Eqs. (13a) and (13b), the energy eigenequations (9a) and (9b) for the atomic SCF Hamiltonian H_0, and the orthogonalization conditions, Eqs. (10a), (10b), and (10c) are used.

In the continuum energy regime and when $E\neq E_n^{(0)}$, the formal solutions of Eqs. (13a) and (13b) [20] are

$$A_n(iE)=\frac{K_{n,iE}N_{iE}}{E-E_n^{(0)}}, \tag{14a}$$

$$B_{i'\epsilon}(iE)=\left[\delta_{ii'}\delta(E-\epsilon)+\mathrm{P}\frac{K_{i'\epsilon,iE}}{E-\epsilon}\right]N_{iE}, \tag{14b}$$

where P indicates the principal integral and N_{iE} is a normalization factor which will be derived in the Appendix. The first term on the right-hand side of Eq. (14b) represents the incident wave from channel i with energy E. Substituting Eqs. (14a) and (14b) into Eqs. (13a) and (13b), we obtained the Lippmann-Schwinger type equations,

$$K_{n',jE}=V_{n',jE}+\sum_n \frac{V_{n',n}K_{n,jE}}{E-E_n^{(0)}}+\sum_i \mathrm{P}\int_{\epsilon_c}\frac{V_{n',i\epsilon}K_{i\epsilon,jE}}{E-\epsilon}d\epsilon, \tag{15a}$$

$$K_{j'E',jE}=V_{j'E',jE}+\sum_n \frac{V_{j'E',n}K_{n,jE}}{E-E_n^{(0)}}+\sum_i \mathrm{P}\int_{\epsilon_c}\frac{V_{j'E',i\epsilon}K_{i\epsilon,jE}}{E-\epsilon}d\epsilon. \tag{15b}$$

Substituting Eqs. (14a) and (14b) into Eq. (11), the continuum wave function for a specific incident wave φ_{iE} is

$$\Psi_{iE}=\sum_n \frac{K_{n,iE}N_{iE}}{E-E_n^{(0)}}\varphi_n+\sum_{i'} \mathrm{P}\int_{\epsilon_c}\frac{K_{i'\epsilon,iE}N_{iE}}{E-\epsilon}\varphi_{i'\epsilon}d\epsilon+\varphi_{iE}N_{iE}. \tag{16}$$

The first and second terms on the right-hand side of Eq. (16) respectively represent the resonance component and the scattering waves for the specific incident wave φ_{iE}. It should be noted that the eigenvectors Ψ_{iE} $(i=1,2,\ldots)$ corresponding to different incident channels are not mutually orthogonal. The eigenvectors corresponding to the same incident channel can be normalized as

$$\langle\Psi_{iE}|\Psi_{iE'})\rangle=\delta(E-E'). \tag{17}$$

The normalization factor N_{iE} is found in the Appendix to be

$$N_{iE}=\left[1+\pi^2\sum_j K_{ji}^2(E)\right]^{-1/2}, \tag{18}$$

where $K_{ji}(E)$ is the on-the-energy-shell element of $K_{j'E',jE}$, namely,

$$K_{ji}(E)=K_{jE,iE}. \tag{19}$$

The asymptotic behavior of the eigenvector Ψ_{iE} at large r is

$$\Psi_{iE}\overset{r\to\infty}{\to}A\left\{\Theta_i\frac{1}{r}\sqrt{\frac{2}{\pi k_i}}\sin\xi_i+\sum_j \Theta_j\frac{1}{r}\sqrt{\frac{2}{\pi k_j}}[-\pi K_{ji}(E)]\cos\xi_j\right\}N_{iE}, \tag{20}$$

which is different from the S-matrix asymptotic behavior used in Refs. [14,21,19]. The asymptotic behavior Eq. (20) causes the total incident wave, which is a superposition of different J^π partial waves, to be a modified plane wave at large r.

To calculate the DR probability, the continuum component of Ψ_{iE} is neglected and only the resonance component is left. Therefore, the dipole transition elements for DR can be expressed as

$$D_{j,\beta\mu}(E)=\langle\Psi_{jE}|P^{(\mu)}|\Psi_\beta\rangle=\sum_n \frac{K_{n,jE}N_{jE}}{E-E_n^{(0)}}\langle\varphi_n|P^{(\mu)}|\Psi_\beta\rangle. \tag{21}$$

C. One discrete state and one continuum state

Consider the situation of one discrete state $(n=1)$ and one continuum $(j=1)$ which have been previously diagonalized, namely, $V_{1,1}=0$ and $V_{1E',1E}=0$. The Lippmann-Schwinger type equations are reduced to

$$K_E=V_E+\mathrm{P}\int_{\epsilon_c}\frac{V_\epsilon K_{\epsilon,E}}{E-\epsilon}d\epsilon, \tag{22}$$

$$K_{E',E}=\frac{V_{E'}K_E}{E-E_\varphi}, \tag{23}$$

where $K_E=K_{1,1E}$, $V_E=V_{1,1E}=V_{1E,1}$, $K_{E',E}=K_{1E',1E}$ and $E_\varphi=E_1^{(0)}$. Substituting Eq. (23) into Eq. (22) leads to

$$K_E=\frac{V_E}{1-\dfrac{F(E)}{E-E_\varphi}}, \tag{24}$$

with

$$F(E)=\mathrm{P}\int_{\epsilon_c}\frac{|V_\epsilon|^2}{E-\epsilon}d\epsilon. \tag{25}$$

Substituting Eqs. (23) and (24) into Eq. (18), the normalization factor is written as

$$N_E=\frac{|E-E_\varphi-F(E)|}{\{[E-E_\varphi-F(E)]^2+\pi^2V_E^4\}^{1/2}}. \tag{26}$$

Thus, the coefficient A_1 of the discrete state φ_1 is obtained,

$$A_1=\frac{K_EN_E}{E-E_\varphi}=\frac{V_E}{\{[E-E_\varphi-F(E)]^2+\pi^2V_E^4\}^{1/2}}. \tag{27}$$

This equation is coincident with Eq. (13) of Ref. [20].

D. Final bound wave functions

Based on the configuration interaction theory, the bound wave function Ψ_β of final states in DR processes can be expanded as

$$\Psi_\beta=\sum_n A_n(\beta)\varphi_n. \tag{28}$$

The coefficients $A_n(\beta)$ are obtained by solving the eigenequation

$$\sum_{n'}[(E-E_{n'}^{(0)})\delta_{nn'}+V_{nn'}]A_{n'}=0. \tag{29}$$

III. CALCULATIONS AND DISCUSSIONS

The calculations start from the determination of the SCF potentials of atomic helium. To make the low orbitals hydrogenic, we generate a SCF potential which is obtained by the self-consistent iteration procedure in a fictitious configuration of $2p_{3/2}^{0.5}3d_{5/2}^{0.5}8k_{15/2}$. This potential makes the $1s$, $2s$, $2p$, $3s$, $3p$, and $3d$ orbitals very close to hydro-

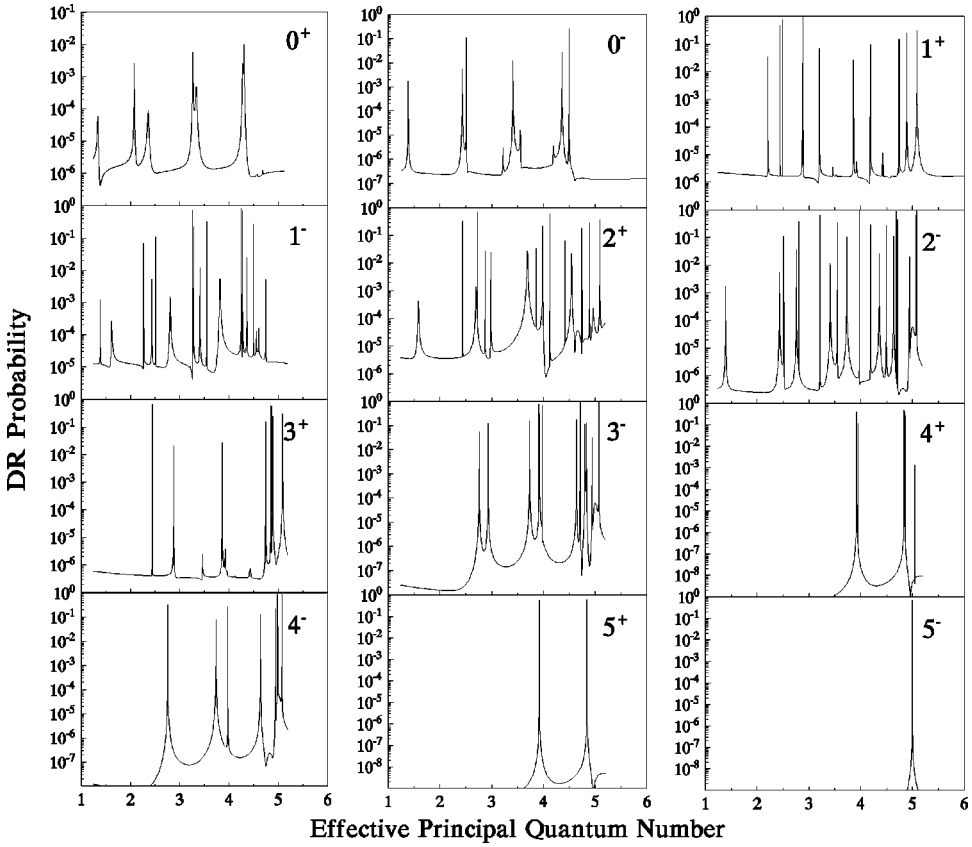

FIG. 1. Partial dielectronic recombination probabilities for He^+ ion in the energy regime of the $2lnl'$ states. The results have included the radiation width by a correction based on isolated resonance approximation.

genic orbitals [9]. All the required bound and continuum orbitals are calculated in this potential.

The channels $1sal_j$, $2sal_j$, $2p_{1/2}al_j$, $2p_{3/2}al_j$, $3sal_j$, $3p_{1/2}al_j$, $3p_{3/2}al_j$, $3d_{3/2}al_j$, and $3d_{5/2}al_j$ are taken into account in the calculations. For each symmetry of the total angular momentum and parity J^π, the quantum number l_j runs over all possible values according to the jj coupling scheme. For bound orbitals, a represents the principal quantum number and runs from $l+1$ to 6 in each channel. For continuum orbitals, a represents orbital energy and takes 15 values from 0.02 to 20 a.u. in each channel. The low limit ϵ_c of the integral for each channel in Eq. (16) takes the value of the middle energy between the states with the principal quantum numbers 5 and 6. The basis wave function φ_n with the principal quantum number 6 is normalized to $\delta(\epsilon - E_n^{(0)})$. Therefore, all the Rydberg basis states with a principal quantum number greater than five are taken into account in the integral.

To resolve the resonance states in each symmetry J^π, the total energy E is scanned. The effective principal quantum number ν of the first closed channel is used to control the energy step. We take $\Delta\nu = 0.01$ as a basic step which is the upper limit of the real step. The real step is autoadjustable to insure that the difference between the DR cross section in the neighbor points is less than 7.5%. With this scheme, some very narrow and strong resonance states are resolved in the energy regime of the $2lnl'$ states. This results in an overestimate of the total DR probability, since the radiation width is neglected in the calculations [8]. A correction for the original DR probability $P^{DR}(E)$ is adopted in the regime

$$\overline{P}^{DR}(E) = P^{DR}(E)\frac{(E-E_0)^2 + \frac{1}{4}A^2}{(E-E_0)^2 + \frac{1}{4}(A+R)^2}.$$

The Auger rate A, radiative rate R, and position E_0 for each resonance state are obtained by fitting the DR probability $P^{DR}(E)$ to

$$P^{DR}(E) = \frac{AR}{(E-E_0)^2 + \frac{1}{4}A^2}$$

in the vicinity of the specific resonance state. In the energy regime of the $3lnl'$ states, there are no narrow and strong resonance states found. This is because of the existence of the $2l\epsilon l'$ Auger channels. The rates of Auger decay of the $3lnl'$ states through these channels are very large. This makes the radiation width negligible compared with Auger width.

In order to compare with experimental measurements directly, the calculated DR cross sections are convolved with the electron distribution of the pseudo-Maxwellian [22] with the vertical temperatures $T_\perp$ and the longitudinal temperature $T_\parallel$. $T_\perp$ and $T_\parallel$ are determined from a fit to the observed shape of the DR resonances. Corresponding to Ref. [10], $T_\perp$ and $T_\parallel$ are equal to 0.15 eV and 0.8×10^{-4} eV, respectively.

The DR cross sections for 12 partial waves with the total angular momentum from 0 to 5 in both parities are calculated in the energy regime where $2lnl'$ doubly excited states lie. The corrected partial DR probabilities are shown in Fig. 1. The resonance states vary periodically with the effective principal quantum number ν except for some very narrow states. The omission of narrow states due to the present scan step of energy have negligible effect on the total DR probability. In the higher ν part, more resonance states appear as more angular momenta are possible. The corresponding convolved partial cross sections are shown in Fig. 2. The mag-

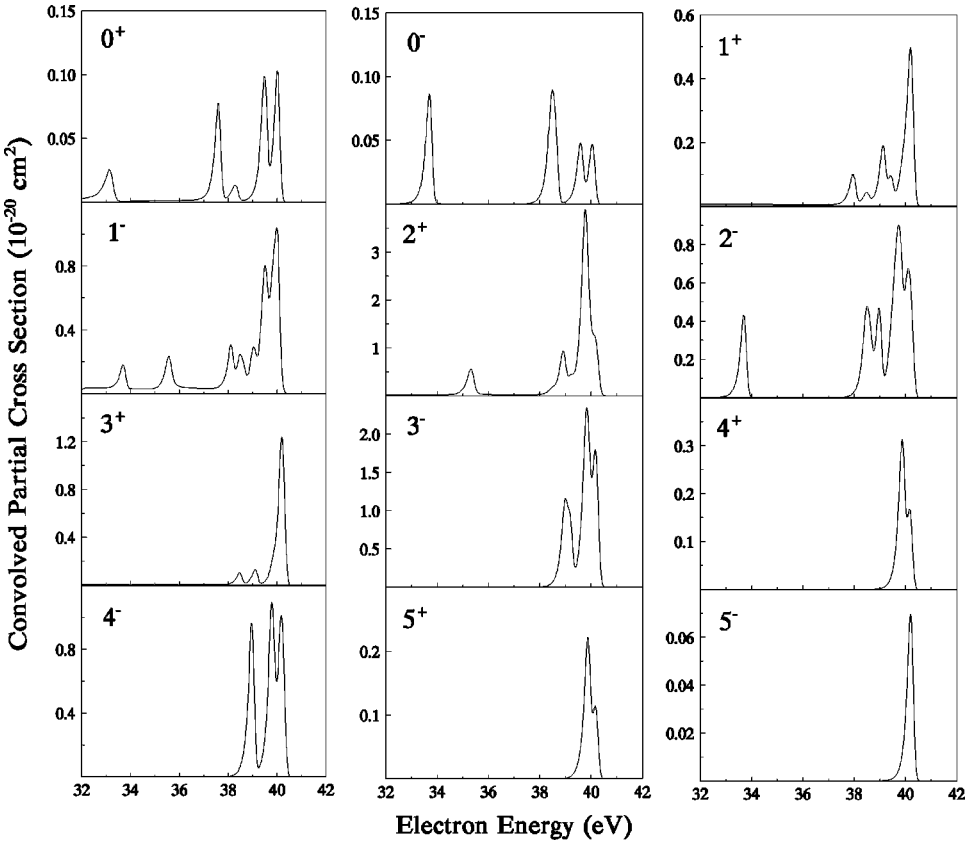

FIG. 2. Convolved partial dielectronic recombination cross sections corresponding to Fig. 1. A pseudo-Maxwellian distribution with the vertical temperatures $T_\perp = 0.15$ eV and the longitudinal temperature $T_\parallel = 0.8\times10^{-4}$ eV is used.

nitude of partial cross sections near 40 eV in decreasing order are from 2^+, 3^-, 3^+, 4^-, 2^-, and 1^+ symmetries. The other partial waves contribute less to the total cross section. The total convolved cross sections are shown in Fig. 3 along with the experimental results of DeWitt *et al.* [10]. For the $2lnl'(n\leqslant3)$ states, the calculated results are in excellent agreement with those of experiment. For the $2l4l'$ states, the calculated position agrees with that of the observation, except that it is higher and wider. For the $2l5l'$ states, the height and position of the calculated peak agree with the experimental ones, but are narrower.

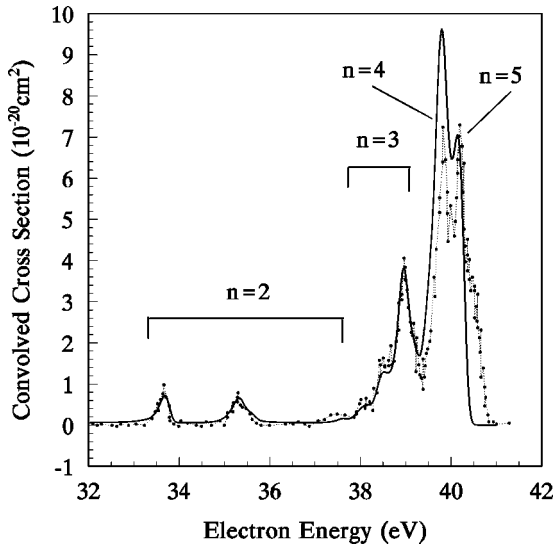

FIG. 3. Comparison of the convolved dielectronic recombination cross section with the experimental measurement for the $2lnl'$ states of He.

Figure 4 shows the calculated partial DR probabilities in the energy regime of the $3lnl'$ states. The values are much smaller than those of the $2lnl'$ states since the $2l\epsilon l'$ Auger channels are possible for the $3lnl'$ states. Figure 5 shows the convolved partial cross sections in this energy regime. Only six partial waves with $J^\pi = 1^-$, 2^+, 2^-, 3^+, 3^-, and 4^- contribute significantly to the DR cross sections. The situation in this energy regime is more complicated than that in the $2lnl'$ states regime since more open channels exist. The $3lnl'$ doubly excited states can decay radiatively to both the $1snl$ bound states and $2lnl'$ lower-lying doubly excited states. The atoms in such states decaying to the bound states contribute to the DR cross section in the experiment. The atoms decaying to the lower-lying doubly excited states $2lnl'$ may undergo a further radiative decay to some bound states and then be recorded by the detector. Another competitive decay path for the $2lnl'$ states is the Auger process. The atoms undergoing an Auger decay could not contribute to the DR cross sections in the experiment. Since the Auger decay is dominant for the doubly excited states of helium, the $3lnl'$ doubly excited states that decay through $2lnl'$ states will rarely contribute to the DR cross sections. In the calculations we only include the bound states $1snl$ as the final states and neglect the cascade effect through $2lnl'$ states. Figure 6 shows the convolved total cross sections in this energy regime along with the experimental data. Similarly to the $2lnl'$ states regime, for the $3l3l'$ states, the calculated results are in good agreement with those of experiment. For the $2l4l'$ states, the calculated peak is wider on the high-energy side than that of observation. For the $3l5l'$ states, the calculated peak is a factor of two higher than that of the experimental one.

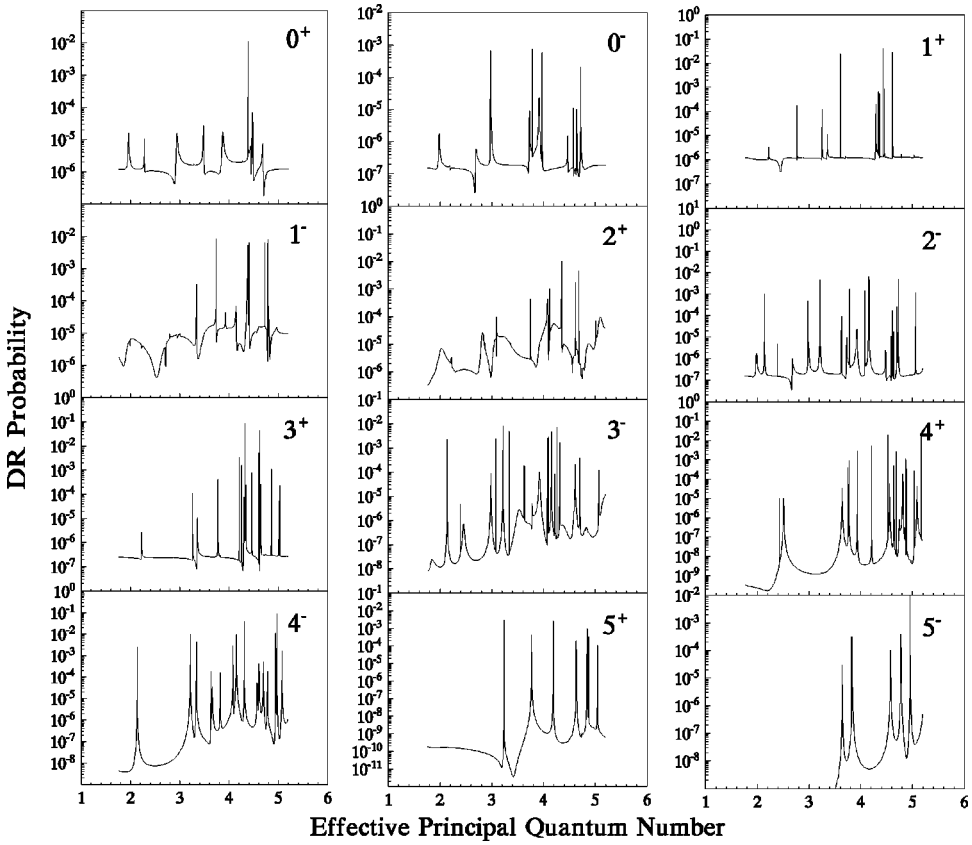

FIG. 4. Similar to Fig. 1, but for the $3lnl'$ states and without the correction.

The discrepancy for $2lnl'$, $3lnl'$ $(n=4,5)$ states may be attributed to the existence of the static external field. In the experiment [10], a static magnetic field was used to select the ions with different charges. The moving atoms or ions felt a static electric field. The states that can survive field ionization were supposed to be those with $n \leqslant n_{max} \approx 5$. As Badnell analyzed [23], the initial field-ionized state is not only n dependent, but also l dependent. The tightly bound lower-l

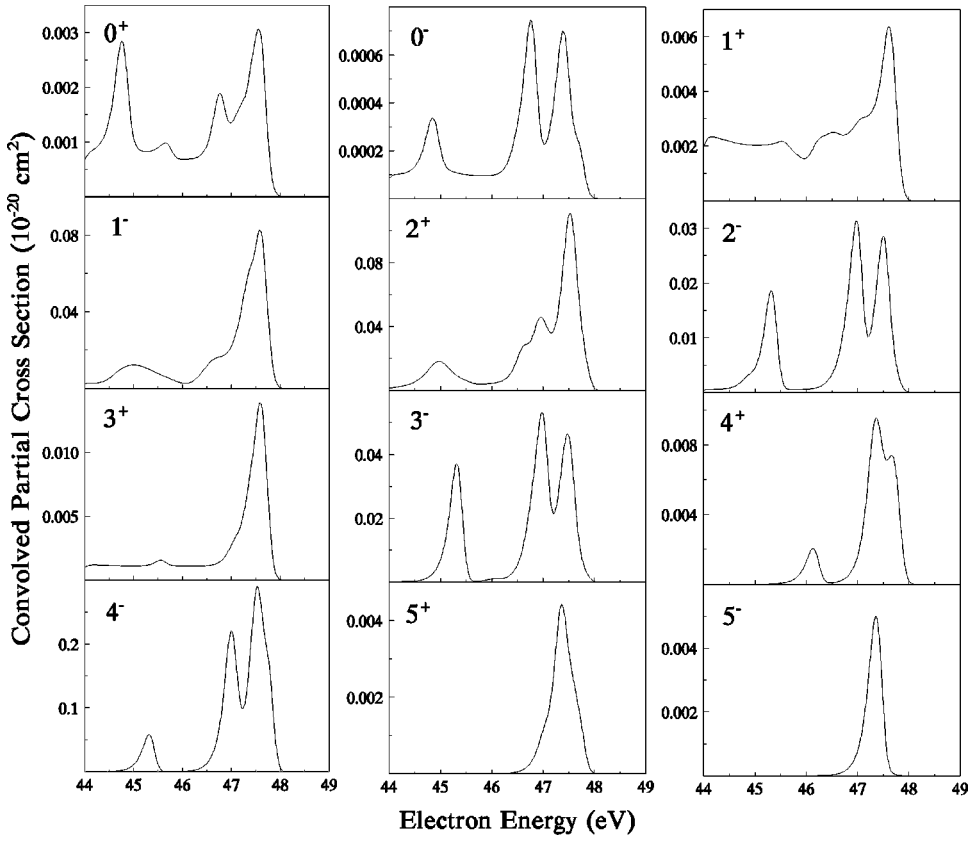

FIG. 5. Similar to Fig. 2, but for the $3lnl'$ states.

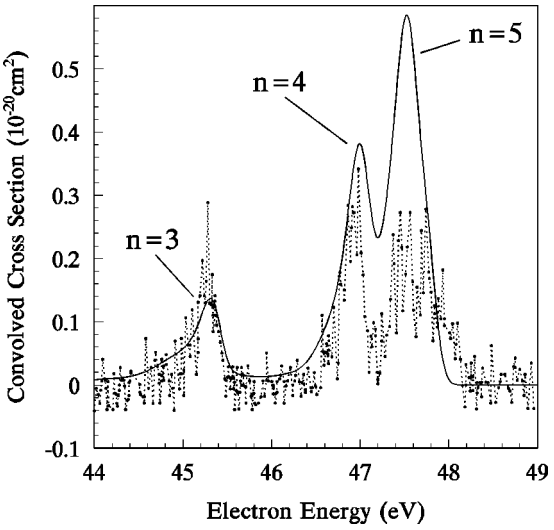

FIG. 6. Similar to Fig. 3, but for the $3lnl'$ states.

states with $n=4$ cannot be field ionized but the loosely bound high-l states can be. Therefore, the DR cross sections for the $2l4l'$ and $3l4l'$ states are overestimated in the present calculations as all the possible l' are taken into account. On the other hand, recombination into the states with n greater than n_{max} can survive field ionization if the outer electron radiates to a final state below n_{max} during the time-of-flight from the cooler to the analyzer. For the $2l5l'$ states, although the DR cross sections are overestimated in the calculations the field-ionizing survival states with $n>n_{max}$ compensate the field ionized part of the $2l5l'$ states in the experiment. The $3l5l'$ states seem being bound more loosely than the $2l5l'$ states. More $3l5l'$ states are field ionized and the states with $n>n_{max}$ can not compensate the lost. The wider side in experimental results at the high-energy part near both the $2l5l'$ and $3l5l'$ states may be due to the states with $n>n_{max}$ also.

IV. CONCLUSIONS

We have calculated the dielectronic recombination cross sections of He^+ for the $2lnl'$ and $3lnl'$ resonance states with $n\leqslant 5$. The results for resonance states with $n\leqslant 3$ in both energy regimes are in good agreement with those of the observations. The discrepancy for the $n=4$ and 5 resonance states may attributed to the l dependence of the field ionization and the radiative decay of the $n>n_{max}$ resonance states to the states with $n<n_{max}$ during the time of flight. It is demonstrated that the accurate atomic wave functions in the continuum energy regime can be obtained by the relativistic multichannel theory. Although the resolution of very narrow resonances without radiation damping overestimates the DR cross sections, a correction based on the isolated resonance approximation is possible as the resonances do not interfere with others. The physical parameters (eigenchannel quantum defect μ_α, transformation matrix $U_{j\alpha}$) of multichannel quantum defect theory can be obtained in the same calculations. The present results also confirmed the reliability of the calculated parameters (μ_α, $U_{j\alpha}$), which can be applied to the study of DR for the high-n Rydberg resonance states based on the theory of Bell and Seaton [16].

ACKNOWLEDGMENTS

One of the authors (Y.Z.) wishes to thank Professor J. M. Li, Dr. N. R. Badnell, and Dr. J. G. Wang for their helpful discussions. This work was supported by the National Science Foundation of China, and it was also partially supported by National High-Tech ICF Committee in China, Science and Technology Funds of CAEP, and National Scientific Youth Fund of Laser Technology.

APPENDIX

Substituting Eq. (11) into Eq. (17) gives the normalization condition as

$$\sum_n A_n(E,i)A_n(E',i)+\sum_j \int B_{j\epsilon}(E,i)B_{j\epsilon}(E',i)d\epsilon = \delta(E-E'). \tag{A1}$$

Using the formal solutions of Eqs. (14a) and (14b) for $A_n(E,i), B_{j\epsilon}(E,i)$ leads to

$$N(E,i)N(E',i)\left\{\sum_n \frac{K_{n,iE}K_{n,iE'}}{(E-E_n^0)(E'-E_n^0)}+\frac{K_{iE',iE}}{E-E'}-\frac{K_{iE,iE'}}{E-E'} + \delta(E'-E)+\sum_j \mathcal{P}\int \frac{K_{j\epsilon,iE}}{(E-\epsilon)}\frac{K_{j\epsilon,iE'}}{(E'-\epsilon)}d\epsilon\right\} = \delta(E-E'). \tag{A2}$$

The factor $1/[(E-\epsilon)(E'-\epsilon)]$ can be resolved into a partial fraction plus a singular term [20] according to

$$\frac{1}{(E-\epsilon)(E'-\epsilon)}=\frac{1}{(E-E')}\left(\frac{1}{E'-\epsilon}-\frac{1}{E-\epsilon}\right) + \pi^2\delta(E-E')\delta\left[\epsilon-\frac{1}{2}(E+E')\right]. \tag{A3}$$

Substituting Eq. (A3) into Eq. (A2), we obtain

$$N(E,i)N(E',i)\left\{Y+\left[1+\pi^2\sum_j K_{ji}^2(E)\right]\delta(E-E')\right\} = \delta(E-E'), \tag{A4}$$

where

$$Y=\sum_n \frac{K_{n,iE}K_{n,iE'}}{(E-E_n^0)(E'-E_n^0)} +\sum_j \mathrm{P}\int \frac{K_{j\epsilon,iE}K_{j\epsilon,iE'}}{E-E'}\left(\frac{1}{E'-\epsilon}-\frac{1}{E-\epsilon}\right)d\epsilon +\frac{K_{iE',iE}}{E-E'}-\frac{K_{iE,iE'}}{E-E'}. \tag{A5}$$

Using the Lippmann-Schwinger equations (15a) and (15b), we will prove that $Y=0$ for $E\neq E'$. Finally, the normalization factor is written as

$$N(E,i)=\left[1+\pi^2\sum_j K_{ji}^2(E)\right]^{-1/2}, \tag{A6}$$

with $K_{ji}(E)=K_{jE,iE}$.

Next we will prove that $Y=0$ using the Lippmann-Schwinger equations. Multiplying both sides of Eq. (15a) with $K_{n,i'E'}/(E'-E_n^0)$ and summing over n lead to

$$\begin{aligned}\sum_n \frac{K_{n,i'E'}K_{n,iE}}{E'-E_n^0}&=\sum_n \frac{K_{n,i'E'}V_{n,iE}}{E'-E_n^0}+\sum_{nn'}\frac{K_{n,i'E'}}{E'-E_n^0}\\&\times\frac{V_{n,n'}K_{n',iE}}{E-E_{n'}^0}\\&+\sum_{j'}\mathrm{P}\int\left(\sum_n\frac{V_{j'\epsilon',n}K_{n,i'E'}}{E'-E_n^0}\right)\\&\times\frac{K_{j'\epsilon',iE}}{E-\epsilon'}d\epsilon'.\end{aligned} \tag{A7}$$

Here $V_{j'\epsilon',n}=V_{n,j'\epsilon'}$ is used in the third term of the right-hand side. Substituting Eq. (15b) into the third term of the right-hand side of the above equation, one obtains

$$\begin{aligned}\sum_n \frac{K_{n,i'E'}K_{n,iE}}{E'-E_n^0}&=\sum_n \frac{K_{n,i'E'}V_{n,iE}}{E'-E_n^0}+\sum_{nn'}\frac{K_{n,i'E'}}{E'-E_n^0}\\&\times\frac{V_{n,n'}K_{n',iE}}{E-E_{n'}^0}\\&+\sum_{j'}\int\frac{K_{j'\epsilon',i'E'}K_{j'\epsilon',iE}}{E-\epsilon'}d\epsilon'\\&-\sum_{j'}\int\frac{V_{j'\epsilon',i'E'}K_{j'\epsilon',iE}}{E-\epsilon'}d\epsilon'\\&-\sum_{jj'}\int\int\frac{V_{j'\epsilon',j\epsilon}K_{j\epsilon,i'E'}}{E'-\epsilon}d\epsilon\frac{K_{j'\epsilon',iE}}{E-\epsilon'}d\epsilon'.\end{aligned} \tag{A8}$$

Commuting the subscripts iE and $i'E'$ in the above equation yields

$$\begin{aligned}\sum_n \frac{K_{n,iE}K_{n,i'E'}}{E-E_n^0}&=\sum_n \frac{K_{n,iE}V_{n,i'E'}}{E-E_n^0}+\sum_{nn'}\frac{K_{n,iE}}{E-E_n^0}\\&\times\frac{V_{n,n'}K_{n',i'E'}}{E'-E_{n'}^0}\\&+\sum_{j'}\int\frac{K_{j'\epsilon',iE}K_{j'\epsilon',i'E'}}{E'-\epsilon'}d\epsilon'\\&-\sum_{j'}\int\frac{V_{j'\epsilon',iE}K_{j'\epsilon',i'E'}}{E'-\epsilon'}d\epsilon'\\&-\sum_{jj'}\int\int\frac{V_{j'\epsilon',j\epsilon}K_{j\epsilon,iE}}{E-\epsilon}d\epsilon\frac{K_{j'\epsilon',i'E'}}{E'-\epsilon'}d\epsilon'.\end{aligned} \tag{A9}$$

Using Eq. (A8) minus Eq. (A9) and considering $V_{n,n'}=V_{n',n}$ and $V_{j\epsilon,j'\epsilon'}=V_{j'\epsilon',j\epsilon}$, one finds,

$$\begin{aligned}\sum_n \frac{K_{n,iE}K_{n,i'E'}(E-E')}{(E-E_n^0)(E'-E_n^0)}&=\sum_n \frac{K_{n,i'E'}V_{n,iE}}{E'-E_n^0}-\sum_n\frac{K_{n,iE}V_{n,i'E'}}{E-E_n^0}\\&+\sum_{j'}\int\frac{K_{j'\epsilon',i'E'}K_{j'\epsilon',iE}}{E-\epsilon'}d\epsilon'\\&-\sum_{j'}\int\frac{K_{j'\epsilon',iE}K_{j'\epsilon',i'E'}}{E'-\epsilon'}d\epsilon'\\&-\sum_{j'}\int\frac{V_{j'\epsilon',i'E'}K_{j'\epsilon',iE}}{E-\epsilon'}d\epsilon'\\&+\sum_{j'}\int\frac{V_{j'\epsilon',iE}K_{j'\epsilon',i'E'}}{E'-\epsilon'}d\epsilon'.\end{aligned} \tag{A10}$$

Using the Lippmann-Schwinger equation again, the above equation is reduced to

$$\begin{aligned}\sum_n \frac{K_{n,iE}K_{n,i'E'}(E-E')}{(E-E_n^0)(E'-E_n^0)}&=K_{iE,i'E'}-V_{iE,i'E'}-K_{i'E',iE}+V_{i'E',iE}\\&+\sum_{j'}\int\frac{K_{j'\epsilon',i'E'}K_{j'\epsilon',iE}}{E-\epsilon'}d\epsilon'\\&-\sum_{j'}\int\frac{K_{j'\epsilon',iE}K_{j'\epsilon',i'E'}}{E'-\epsilon'}d\epsilon'.\end{aligned} \tag{A11}$$

Finally, considering the symmetry property of the V matrix, we get

$$\begin{aligned}\sum_n \frac{K_{n,iE}K_{n,i'E'}(E-E')}{(E-E_n^0)(E'-E_n^0)}&=K_{iE,i'E'}-K_{i'E',iE}\\&+\sum_{j'}\int\frac{K_{j'\epsilon',i'E'}K_{j'\epsilon',iE}}{E-\epsilon'}d\epsilon'\\&-\sum_{j'}\int\frac{K_{j'\epsilon',iE}K_{j'\epsilon',i'E'}}{E'-\epsilon'}d\epsilon',\end{aligned} \tag{A12}$$

and then $Y=0$ for $E-E'\neq 0$.

[1] A. Burgess, Astrophys. J. **139**, 776 (1964); **141**, 1588 (1965).
[2] M. J. Seaton and P. J. Storey, in *Atomic Processes and Applications*, edited by P. G. Burke and B. L. Moiseiwitsch (North-Holland, Amsterdam, 1976) p. 133.
[3] J. Dubau and S. Volonte, Rep. Prog. Phys. **43**, 199 (1980).
[4] Y. Hahn, Adv. At. Mol. Phys. **21**, 123 (1985).
[5] L. H. Andersen, Comments At. Mol. Phys. **25**, 27 (1991).
[6] S. Mannervik *et al.*, Phys. Rev. Lett. **81**, 313 (1998).
[7] A. K. Pradhan and M. J. Seaton, J. Phys. B **18**, 1631 (1985).
[8] N. R. Badnell, T. W. Gorczyca, and A. D. Price, J. Phys. B **31**, L239 (1998).
[9] Yu Zou, Quan-Yu Fang, and Jia-Ming Li, Chin. Phys. Lett. **15**, 175 (1998).
[10] D. R. DeWitt *et al.*, J. Phys. B **28**, L147 (1995).
[11] Jian-Guo Wang, Yi-Zhi Qu, and Jia-Ming Li, Phys. Rev. A **52**, 4274 (1995); Jian-Guo Wang (private communication).
[12] Yu Zou, Xiao-Min Tong, and Jia-Ming Li, Acta Phys. Sin. **44**, 50 (1995).
[13] Wen Huang, Yu Zou, Xiao-Min Tong, and Jia-Ming Li, Phys. Rev. A **52**, 2770 (1995).
[14] P. C. W. Davies and M. J. Seaton, J. Phys. B **2**, 757 (1969).
[15] J. Gau and Y. Hahn, J. Quant. Spectrosc. Radiat. Transf. **23**, 121 (1980).
[16] R. H. Bell and M. J. Seaton, J. Phys. B **18**, 1589 (1985).
[17] K. J. LaGattuta, Phys. Rev. A **38**, 1820 (1988).
[18] S. L. Haan and V. L. Jacobs, Phys. Rev. A **40**, 80 (1989).
[19] F. Robicheaux, T. W. Gorczyca, M. S. Pindzola, and N. R. Badnell, Phys. Rev. A **52**, 1319 (1995).
[20] U. Fano, Phys. Rev. **126**, 1866 (1961).
[21] M. J. Seaton, Rep. Prog. Phys. **46**, 167 (1983).
[22] L. H. Anderson *et al.*, Phys. Rev. Lett. **62**, 2656 (1989).
[23] N. R. Badnell (private communication); D. R. Dewitt *et al.*, Phys. Rev. A **50**, 1257 (1994).